

Electronic structure of molecular van der Waals complexes with benzene: Implications for the contrast in scanning tunneling microscopy of molecular adsorbates on graphite

R. Lazzaroni, A. Calderone, and J. L. Brédas

Service de Chimie des Matériaux Nouveaux, Centre de Recherche en Electronique et Photonique Moléculaires, Université de Mons-Hainaut, Place du Parc 20, B-7000 Mons, Belgium

J. P. Rabe

Department of Physics, Humboldt University Berlin, Invalidenstrasse 110, D-10115 Berlin, Germany

(Received 1 July 1996; accepted 26 March 1997)

We investigate the electronic structure of molecular model systems in order to improve our understanding of the nature of the contrast, which is observed in the scanning tunneling microscopy (STM) imaging of organic adsorbates on graphite. The model systems consist of a benzene molecule, representing the substrate surface, interacting with various molecules representing alkyl chains, oxygen- and sulfur-containing groups, fluorinated species, and aromatic rings. We perform quantum-chemical calculations to determine the geometric structure, stability, and electronic structure of these molecular complexes and analyze the theoretical results in relation with experimental STM data obtained on monolayers physisorbed on graphite. It appears that the STM contrast can be correlated to the energy difference between the electronic levels of the substrate and those of the adsorbate. Finally, we observe that the introduction of a uniform electric field in the quantum-chemical modeling can enhance the electronic interaction between the partners in the complex. © 1997 American Institute of Physics. [S0021-9606(97)00625-9]

I. INTRODUCTION

Scanning tunneling microscopy (STM) has emerged as a remarkable tool to investigate organic molecules on electronically conducting solid substrates with atomic scale resolution.¹⁻³ One particularly appealing substrate is the basal plane of highly oriented pyrolytic graphite (HOPG) because it is chemically inert, and it exhibits very large atomically perfect flat terraces. This allows to study highly ordered molecular monolayers, which interact only weakly with the substrate, and whose electronic structure is therefore only weakly perturbed.

STM experiments have been carried out on monomolecular layers of long alkanes,⁴⁻⁸ as well as on a large series of alkyl derivatives including alkanols,^{5,9} fatty acids,⁵ various alkylated aromatic molecules,^{5,10-14} alkane thiols,¹⁵ and selectively fluorinated fatty acids,¹⁶ immobilized at the interface between organic solutions or melts and the basal plane of HOPG. These data show that the monolayers organize as two-dimensional crystals. Crystal structure and orientation are governed by weak interactions, both between the molecules and the substrate and between the molecules within the layers. Similarly, ordered molecular layers have been formed by sublimation of aromatic molecules in vacuum.^{17,18}

All the experiments referred to above have provided outstanding information on the structure and dynamics of organic monolayers on HOPG. This was possible despite the fact that a good understanding of the origin of the contrast is still lacking, since the conclusions were mainly based on size and symmetry arguments. On the other hand, given the good understanding of molecular structure and dynamics, the same experimental data may also be used in order to investigate

the STM contrast for a variety of molecular segments in well-defined molecular environments. Interestingly, some general trends are apparent from previous work. For instance, for a large variety of alkylated aromatics, constant height images obtained in similar conditions reveal that the current through the aromatic part is generally, considerably larger than through the aliphatic part.¹¹⁻¹⁵ The aim of the work presented in this paper is to contribute to the understanding of such general trends.

Various interpretations for the contrast have been proposed in the literature. On one hand, the contrast has been related to the polarizability of the adsorbed molecule.¹⁰ The presence of a polarizable molecule or molecular fragment in the electric field between the tip and the substrate would locally modify the workfunction of the substrate, hence the barrier height, which would in turn, affect the intensity of the tunneling current. On the other hand, the contrast has also been interpreted in terms of the distribution of the electron density in the frontier molecular orbitals of the adsorbate. Examples include adsorbates at the interface between liquid crystals and graphite,¹¹ phthalocyanines on copper,¹⁹ and substituted alkanes on graphite.²⁰ For the specific case of xenon atoms on nickel, the current has been explained on the basis of a resonance between the empty Xe 7s states (LUMO) and the Fermi surface of the metal.²¹ Recently, the current through alkane and polyene chains has been calculated, taking into account the interaction between substrate and adsorbate with a calculation based on extended Hückel molecular orbitals. The results indicate that the HOMO-LUMO gap has a strong influence on the electron transport properties.²²

In this work, we consider the following model, in order

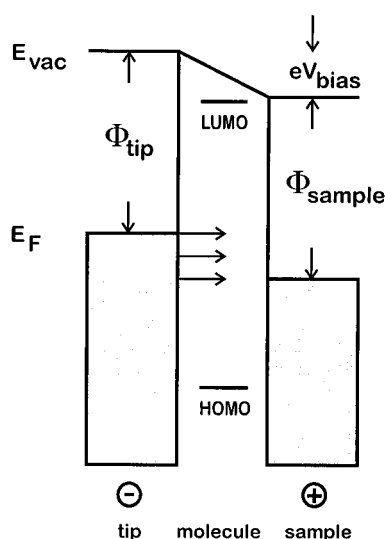


FIG. 1. Schematic energy diagram for a STM junction with a molecule.

to describe the tunneling through various flat-lying alkyl derivatives on HOPG under typically used experimental conditions.^{4–16} Electrons from a metallic STM-tip tunnel through a molecule into the conducting substrate, or vice versa. A schematic energy diagram is displayed in Fig. 1. The workfunctions Φ of the electrodes are around 4 eV, and the applied bias voltage is typically around 1 V. For a weak electronic coupling between substrate and adsorbate (as in the present case), one may expect that the broadening of the molecular states is small and the Fermi energies are roughly in the middle between the HOMO and LUMO. If the HOMO–LUMO gap is larger than the applied bias, the energies of the molecular states are far away from the Fermi energies. However, the experiments show that the tunneling current reflects a distinct difference between alkyl and aromatic segments,^{10–14} which cannot be simply attributed to topography. Therefore, the current must couple to the molecular states. This may be attributed to resonant tunneling through some small density of states within the gap, which is due to the broadening of the molecular levels centered several eV apart, similar to the case of Xe on Ni (Ref. 21) and alkanes on Au.²² One may expect that the density of states derived from the molecule, taken at the Fermi level, increases as the gap between the HOMO (or the LUMO) and the Fermi level decreases, and/or the coupling between substrate and adsorbate increases.

In order to model the interactions between substrate and adsorbate, we use here a quantum-chemical approach based on the *ab initio* Hartree–Fock methodology. We consider the basic structural unit of graphite, benzene, as a model for the substrate, interacting with molecules containing either, carbon, oxygen, sulfur, or fluorine atoms, i.e., CH₄, H₂O, H₂S, and CF₄. The methane molecule is the basic model for methylene units (–CH₂–) in alkyl chains while the other molecules represent the functional groups present in the systems studied experimentally with STM;^{4–16} they will be referred to as the “small molecules”. To investigate the inter-

action between aromatic units, we also consider the benzene dimer. In previous studies, we have examined the geometric structure and some aspects of the electronic structure of a few of these complexes.^{23–25} In this paper, we briefly describe the major geometric features in the whole series and focus on the evolution of the electronic structure, in particular the distribution of the highest valence electronic states in the complexes. We also investigate the influence of an external electric field, corresponding to the bias voltage of the tunneling junction, on the electronic structure of the systems. This paper is organized as follows: the STM results that we aim at understanding are summarized in Sec. II; the theoretical methodology is described in Sec. III. The electronic structure of the complexes and the influence of the external electric field are presented in the next two sections.

II. EXPERIMENTAL OBSERVATIONS

STM on molecular adsorbates is based on electron tunneling from a metallic tip through a molecule into a conducting substrate, or vice versa. In practice, an atomically sharp tip is approached towards the substrate to within a distance small enough that a tunneling current can be measured, i.e., on the order of 1 nm. A convenient mode of operation for very flat surfaces is to scan the tip in a fixed plane across the surface and to record the current at a given bias voltage. The position of the plane relative to the substrate surface is determined by the average tunneling current and the bias. Therefore, it is possible to record current images as a function of bias or tip-sample distance.

Experiments on alkyl derivatives^{9,13,15,16} revealed that, in a bias range of (1.0 ± 0.5) V and at an average current of about 1 nA, the current through the different molecular segments can be calibrated against the current through the alkyl chains; in this way, the spectroscopic information is rather independent from the particular tip. It was found that the current through the sulfur atoms in the thiols [Fig. 2(a)], as well as the current through aromatic segments [Fig. 2(b)], were significantly larger than the current through the alkyl groups; on the other hand, the current through the oxygen functions in alkanols and fatty acids was rather similar to the current through the alkyl chains [Fig. 2(c)]. In the case of the fluorinated compounds, a much smaller current was observed over the fluorinated groups, relative to the rest of the alkyl chain [Fig. 2(d)]. In all these experiments, the organic molecules lie more or less flat on the surface.

These results show that there is a strong dependence of the tunneling current on the chemical nature of the functionalities of the adsorbates, and that a single atom within the adsorbate can dramatically modify the tunneling current. In that sense, these results are reminiscent of the imaging of single Xe atoms physisorbed on metal surfaces.²¹

III. THEORETICAL METHODOLOGY

The geometry of the complexes was optimized with the small molecule lying above the benzene plane, in order to simulate the physisorption on a graphite surface (Fig. 3). The H₂O and H₂S molecules were oriented with the heavy atom

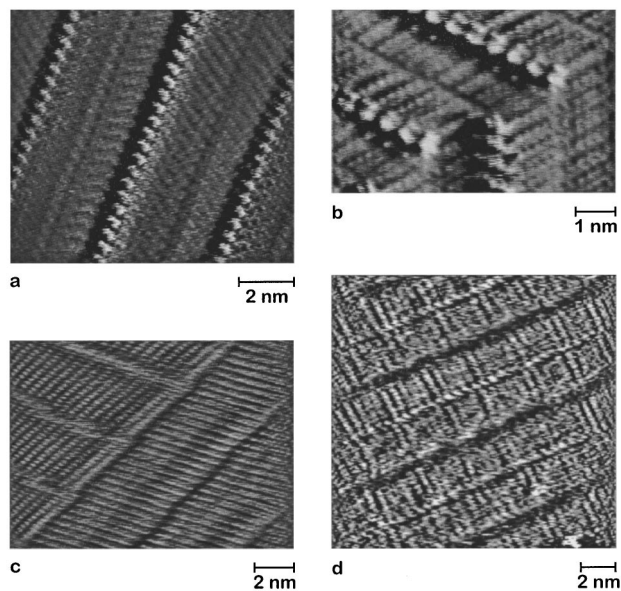


FIG. 2. STM images obtained in the current mode for molecular adsorbates on graphite: (a) dihexadecylsulfide ($-S-S-$) (Ref. 15), (b) didodecylbenzene ($-C_6H_6-$) (Ref. 13), (c) triacontanol ($-OH$) (Ref. 9), and (d) 12-fluorostearic acid ($-F$) (Ref. 16). Brighter areas correspond to larger currents. Note the presence of dark stripes within the lamellae, corresponding to the location of fluorine atoms, in image d. The images were obtained in the current mode in a bias range of (1.0 ± 0.5) V and at an average current of about 1 nA.

lying on the C_6 symmetry axis of benzene and the two protons pointing towards the aromatic ring. This structure corresponds to the configuration observed experimentally in the H_2O /benzene complex.²⁶ In order to limit the computational effort, these complexes were maintained in a C_{2v} configuration during the geometry optimization (note that in the real system, the C_2 axis of the H_2O molecule is slightly tilted relative to the C_6 axis of benzene²⁶).

The CH_4 /benzene and CF_4 /benzene complexes were also constrained in a similar C_{2v} configuration, even though previous calculations and experiments²⁴⁻²⁹ have shown that the most favorable orientation for CH_4 (CF_4) is with three hydrogen (fluorine) atoms directed towards the benzene molecule. In this work, we have chosen to put only two hydrogens (fluorine) atoms closer to benzene in order to better simulate the interaction between a $-CH_2-$ ($-CF_2-$) group and the graphite surface. For the benzene dimer, most calculations have been performed on the perpendicular ‘‘T-shaped’’ configuration, as it is very close to the experimental structure;³⁰ this is also the most stable configuration found in theoretical calculations including electron correlation³¹ (we note that the parallel displaced configuration is also possible; its consideration does not lead to significant electronic structure modifications due to the overall weakness of the interactions²⁵).

The geometry optimization of the complexes was carried

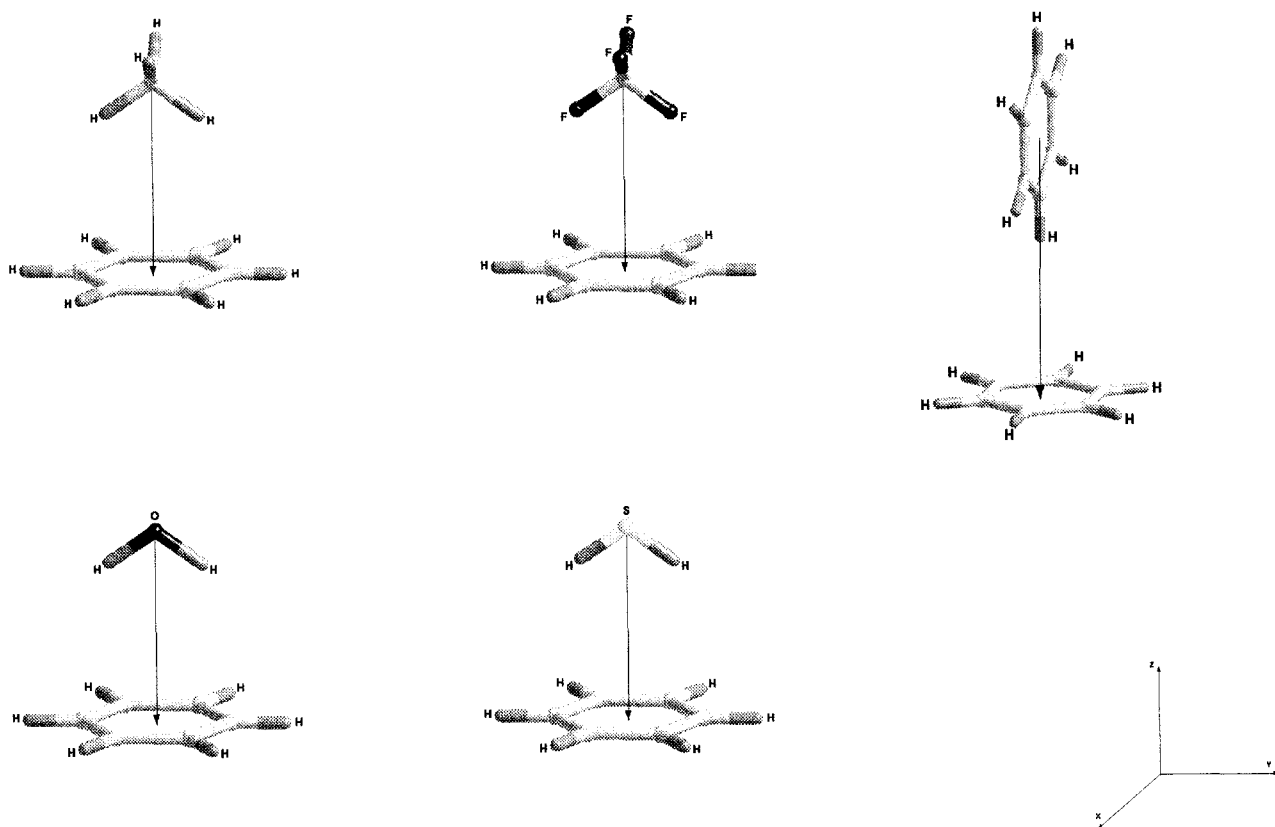


FIG. 3. Geometric structure of the complexes; clockwise from top left: CH_4 /benzene, CF_4 /benzene, the benzene dimer, H_2S /benzene, and H_2O /benzene.

out in two steps. First, a full optimization was performed on the isolated molecules. Then, the two molecules of a given complex were brought together in the configuration described above and the intermolecular distance was optimized with the intramolecular structures kept frozen. This was done on the basis of preliminary calculations which showed that the formation of the complex does not affect significantly the internal geometry of the partners. The validity of this approach is also confirmed by the fact that in HF/ethylene and HF/acetylene complexes, the bond lengths calculated in the complexes have been found to be within 0.005 Å of the values obtained in the isolated molecules.³²

All calculations were performed at the *ab initio* restricted Hartree–Fock level with the HONDO-8 software package³³ running on an IBM/RISC 6000 workstation. We adopted the same methodology as that successfully used in previous similar instances:^{23–25} the geometry optimizations were carried out with a 3–21 G split-valence basis set (RHF/3–21 G); the electronic properties of the optimized structures were then calculated with a 6–31 G* basis set including polarization functions on nonhydrogen atoms. We stress that in such systems, it has been found earlier that RHF/3–21 G geometries are reasonable in comparison to MP2/6–31 G* geometries,^{23,24} therefore, since we are interested in the one-electron structure and not in the binding energies, we kept the RHF approach. We also considered the influence of a homogeneous external electric field, set parallel to the symmetry axis of the systems (which goes through the central atom of the small molecule and the center of the benzene plane). The origin of the coordinates was set at the center of mass and the magnitude of the field was chosen to correspond approximately to the fields present in a STM experiment, typically on the order of 0.1 V/Å. Again, the geometry was optimized at the RHF/3–21 G level and the electronic properties calculated with the RHF/6–31 G* technique.

IV. GEOMETRIC AND ELECTRONIC STRUCTURE OF THE COMPLEXES

The optimized distance between the central atom of the small molecule and the benzene plane is 4.048 Å for CH₄/benzene, 3.397 Å for H₂O/benzene, 3.841 Å for H₂S/benzene, and 3.917 Å for CF₄/benzene. For the benzene dimer in the T configuration, the distance between the centers of the two molecules is 5.300 Å. Compared to theoretical calculations performed with a 6–31 G* basis set, including electron correlation via Møller–Plesset second-order (MP2) perturbation theory,²⁴ the intermolecular distances found here are in general overestimated by 0.2–0.3 Å, this is a direct consequence of neglecting electron correlation, since the dispersive part of the interaction is not properly taken into account. We also have to stress that the intermolecular potentials are extremely flat over a wide range of intermolecular distances around the optimum.²⁴ We can thus consider the present results as satisfactory in the present context since, as indicated above, the scope of this work is to understand the evolution of the electronic structure of the complexes in the series, rather than to determine their exact geo-

metrical parameters: the electronic structure is not modified in any significant way if the intermolecular distances are lowered by 0.2–0.3 Å.

The binding energies for the complexes between the small molecules and benzene are small, on the order of 2–5 kcal/mol.^{23–29,34} This clearly indicates that only weak interactions are at work between the partners, hence, these systems are often called van der Waals complexes.³⁵ Again, from such small binding energies, we expect that complex formation is not to significantly affect the intrinsic one-electron energy levels of the partners, as will be discussed below.

Besides permanent dipole-induced dipole interactions (as in H₂O/benzene) and induced dipole-induced dipole interactions (in all complexes), another phenomenon playing a role in the stability of most of the complexes is the presence of a small but significant charge transfer from benzene to the small molecules. The charge transfer, as obtained from a Mulliken population analysis, is calculated to be on the order of 0.01 |*e*| (see Fig. 6); it can be understood as being the result of hydrogen bonding between the small molecule and the π system of benzene, acting as proton donor and proton acceptor, respectively. This phenomenon, which has been observed experimentally in H₂O/benzene,²⁶ appears to be a general feature in this series of complexes when the small molecule carries hydrogen atoms. The charge transfer is expectedly strongest (~0.015|*e*|) towards the most polar molecules (H₂O and H₂S). Obviously, no such hydrogen bonding is established between benzene and CF₄; in that case, a small charge transfer (~0.003|*e*|) is observed from the electron-rich fluorine atoms to the aromatic ring.

With the analysis of the electronic structure of the complexes, our purpose is determining how the molecular electronic states localized on the isolated molecules are affected by the formation of the van der Waals complexes, in order to understand what the electronic interactions are between the adsorbates and the graphite plane. In this context, we only examine the occupied valence states, for which the RHF/6–31 G* method should provide reliable results, and we neglect the unoccupied states, which are not described accurately at the Hartree–Fock level. Our results are therefore more relevant to the modeling of tunneling experiments in which electrons flow from the occupied states of the sample to the tip. Note, however, that the STM measurements on the adsorbed monolayers are found to be insensitive to the bias polarity.

Since intermolecular interactions are relatively weak in the complexes, the wave functions associated with the one-electron levels of the partners tend to mix only very slightly. Thus, the electronic states of the complexes can generally be considered as localized on one or the other molecule, based on the analysis of the linear combination of atomic orbitals (LCAO) coefficients.

The electronic structure of the five complexes is schematically shown in Fig. 4. The molecular levels centered on the small molecules correspond to F 2*p* lone pairs and C 2*p*–F 2*p* states, C 2*p*–H 1*s* states, O 2*p*–H 1*s* states and oxygen lone pairs, and S 3*p*–H 1*s* states and sulfur lone

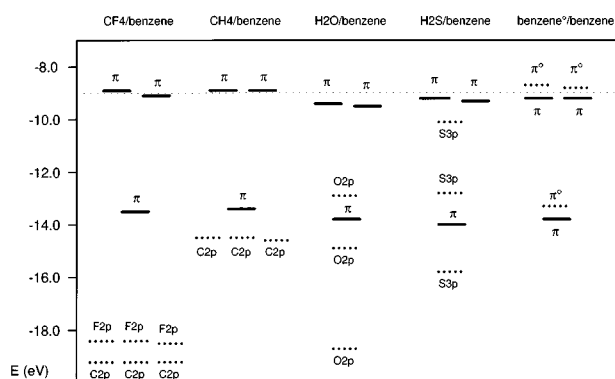


FIG. 4. Electronic structure of the complexes (RHF/6–31 G* values). Only the most relevant electronic levels of benzene (full lines) and the small molecules (dotted lines) are shown. The horizontal broken line at 9.0 eV corresponds to the position of the HOMO of the isolated benzene molecule.

pairs in CF₄/benzene, CH₄/benzene, H₂O/benzene, and H₂S/benzene, respectively (for convenience, these levels are hereafter referred to as F 2*p*, C 2*p*, O 2*p*, and S 3*p*, respectively). The highest-occupied molecular orbital (HOMO) of the complexes always corresponds to the HOMO of benzene. While in isolated benzene, the HOMO is doubly degenerate and is calculated to appear at -9.00 eV, the intermolecular interactions existing in the complexes lift this degeneracy by a few hundredths of an eV. A more important effect is the stabilization of the highest two levels of benzene upon complex formation. This effect is related to the strength of the interaction between the partners, in the sense that it correlates well with the binding energy: while the stabilization is only 0.02 eV in CH₄/benzene (binding energy around 2 kcal/mol^{23–25}), it increases to ≈ 0.4 eV in H₂O/benzene [binding energy around 5 kcal/mol (Refs. 23–25)]. The effect can also be understood as a result of the charge transfer towards the small molecule, which reduces the electron density on the π system. Consistent with the evolution of the benzene levels, the formation of the complex also leads to a 0.2–0.4 eV destabilization of the molecular levels of the small molecules. For instance, the HOMO of H₂S shifts from -10.47 eV in the isolated molecule to -10.10 eV in the complex. As expected, in the benzene dimer, four levels appear near -9 eV, those of the “substrate” ring being slightly stabilized due to the interaction with one proton of the “adsorbed” ring.

Very importantly, a marked difference in the relative positions of the levels of benzene and the small molecules appears from Fig. 4. The molecular orbitals localized on CF₄ are very far in energy (≈ 10 eV) from the HOMO of the complex. This energy difference decreases for the complexes with CH₄ and H₂O, as the highest C 2*p* and O 2*p* levels lie in the 4–5 eV range from the HOMO, and it becomes very small in H₂S/benzene, where the highest level of H₂S lies only 0.8 eV below the levels of benzene. Obviously, the difference is even smaller in the benzene dimer. A detailed LCAO analysis indicates that in the latter two complexes, the levels are close enough in energy for the corresponding wave

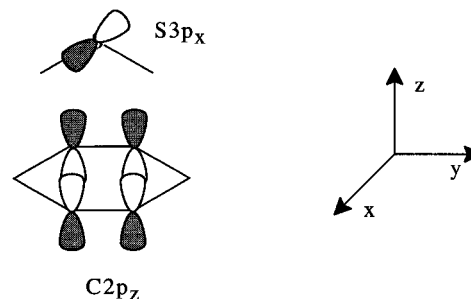


FIG. 5. Sketch of the most significant LCAO coefficients in the HOMO of the H₂S/benzene complex.

functions to interact significantly; as a result, the highest-occupied electronic level of these complexes possesses a contribution from the “adsorbed” molecule, as sketched in Fig. 5.

The major aspect of these results is that the evolution in the electronic structure described in Fig. 4 qualitatively parallels the experimental STM observations: fluorinated groups, in which the electronic states are very distant from those of the substrate, give rise to very low currents; the signal from alkyl chains and oxygen-containing species (represented here by CH₄ and H₂O) is intermediate; and strong tunneling currents are measured above sulfide groups and aromatic rings, for which there occurs a significant electronic interaction with the substrate. This picture is also consistent with the bias-dependent STM images of the adsorbates. In the case of pure alkane layers, at low bias, only the underlying structure of graphite is observed and the molecular lamellae only appear when the bias is raised above certain values.¹⁵ Similarly, when dialkylbenzenes are imaged at low bias, only the phenyl rings are visible and it takes a bias increase to image the full molecule. All these results are consistent with a model in which the tunneling current increases as the energy gap between the electronic levels of the adsorbate and of the substrate decreases.

Finally, it is worth pointing out that the calculated values of the polarizability of the complexes do not support a model relating the STM contrast to local variations in the workfunction of the system due to the presence of polarizable adsorbates.¹⁰ Except for the high value of the benzene dimer ($\alpha_{zz} = 14.6 \text{ \AA}^3$), which is due to its particular geometry, all the complexes show comparable polarizabilities. The H₂O/benzene system has the lowest value (4.4 \AA^3), even lower than CF₄/benzene (4.9 \AA^3), while the CH₄ complex is closer to H₂S/benzene (5.6 and 6.1 \AA^3 , respectively).

V. INFLUENCE OF AN EXTERNAL ELECTRIC FIELD

The geometry optimizations carried out in the presence of an electric field with a magnitude ranging from -0.004 to $+0.004$ atomic units (i.e., from -0.2 to $+0.2$ V/Å; 1 a.u. of field = 5.14×10^{11} V/m) lead to no significant modifications relative to the zero-field molecular structures, both in intramolecular and intermolecular distances. This behavior is in agreement with studies performed on simple hydrocar-

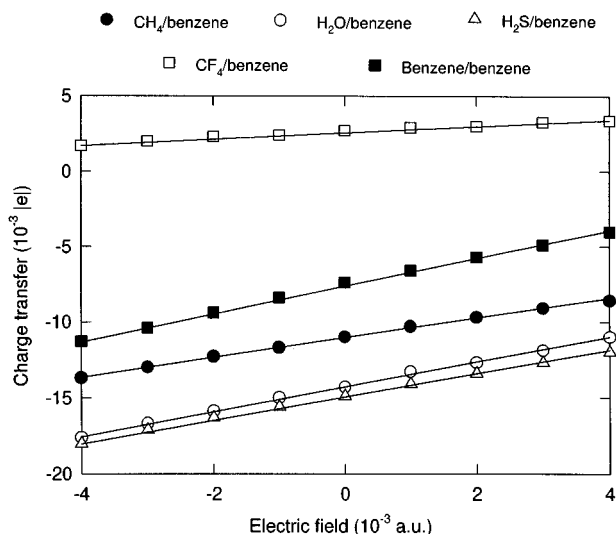


FIG. 6. Charge transfer between benzene and the small molecules as a function of the electric field (RHF/6–31 G* values). Negative values correspond to an increase of the electron density on the small molecule.

bons, NH₃ and CO, which show that much stronger fields, on the order of 0.02 a.u., are necessary to induce significant changes in the geometry.³⁶ The evolution of the total (Stark) energy (*I*) as a function of the electric field (not shown here) follows a second-order dependence, as expected for the low field values used here:

$$E(F) = E_0 - \sum_i \mu_{0i} F_i - \frac{1}{2} \sum_{ij} \alpha_{ij} F_i F_j \quad (1)$$

$$\mu_i(F) = \mu_{0i} + \sum_j \alpha_{ij} F_j = - \frac{\delta E(F)}{\delta F_i} \quad (2)$$

In the above equations, *E* is the total energy of the system, *E*₀ being the zero-field value; *F*_{*i*} is the component of the electric field along the *i* direction; *μ*_{*i*} is the dipole moment along the *i* direction, *μ*₀ being the zero-field value; *α*_{*ij*} is the *ij* element of the linear polarizability tensor.

Following these two equations, the system is most destabilized, i.e., the total energy is maximum, for the value of the field which brings the dipole moment to zero. This maximum destabilization is only observed for the CH₄/benzene and CF₄/benzene complexes, since the field range we consider is not sufficient to suppress the dipole moment in the H₂O and H₂S complexes. Nevertheless, we find that depending on the sign of the electric field, the charge transfer between the partners is significantly different (note that we take a negative field along the C₆ axis of benzene to correspond to the negative pole being on the side of benzene and the positive pole on the side of the small molecule). Figure 6 shows the evolution of the charge transfer as a function of the external field for the various complexes. In all cases, a linear relationship is observed over the field range considered. Since the intermolecular distances are found to remain constant upon application of the field, the degree of charge transfer can be considered to be directly proportional to the dipole moment.

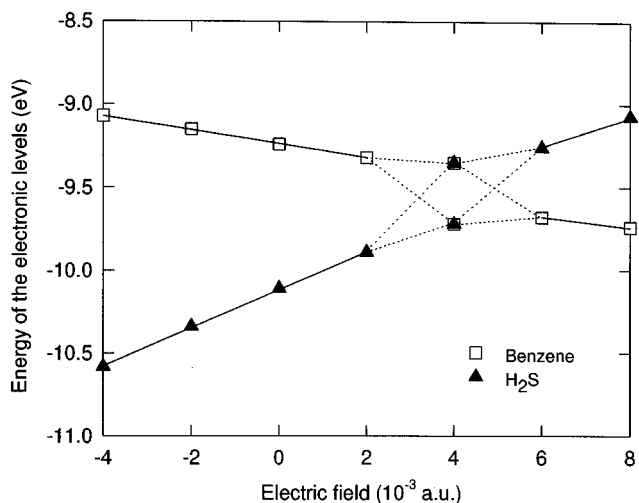


FIG. 7. Energy of the highest-occupied electronic level of benzene (open squares) and the highest S 3*p* level of H₂S (crosses) in the H₂S/benzene complex as a function of the electric field (RHF/6–31 G* values).

Therefore, the linear dependence observed here is simply a consequence of the relation expressed in Eq. (2) and the differences in the slopes of the curves reflect the difference in the polarizability of the complexes.

Most important, the electric field can strongly influence the electronic structure of the uppermost valence levels. A dramatic case is benzene/H₂S. Figure 7 shows the evolution of the energies of the HOMO of benzene and of the S 3*p* uppermost level. At negative and zero-electric fields, the benzene level clearly constitutes the HOMO of the system. The two levels then come closer as the field becomes more positive. The analysis of the LCAO coefficients of the HOMO wave function at *F* = +0.004 a.u. indicates that the characteristics of the two levels intimately mix for that value of the field. Extending the calculations towards higher fields leads to the complete crossing of the two states: the HOMO of the complex now corresponds to a S 3*p*-based level while the *π* levels of the aromatic unit are located at lower energies. The same type of behavior is also observed for the benzene dimer.

For the other complexes, applying the electric field basically has the same effect on the electronic structure: positive fields tend to destabilize the electronic levels of the small molecule while stabilizing the HOMO of benzene. For instance, the highest C 2*p*–H 1*s* level of CH₄ is destabilized by 0.4 eV for a +0.004 a.u. field while the HOMO of benzene shifts down by 0.2 eV. However, due to the large zero-field energy difference between those two levels, no electronic interaction is observed in this field range and the two states do not mix.

Again, these results are consistent with the fact that sulfide groups and aromatic groups can be imaged at low bias (corresponding to small electric fields) while the other groups can only be seen at higher biases (corresponding to higher electric fields).

VI. CONCLUSIONS

The quantum-chemical study of small molecules interacting with benzene, as models for the adsorption of organic molecules on graphite, has shown that there is a qualitative correlation between the STM contrast and the energy separation between the electronic levels of the substrate and the adsorbate. The groups which possess upper-lying electronic states close to those of benzene, such as thiol and phenyl, give rise to a strong current. When the difference becomes a few eV, as for hydroxy or alkyl, the current is intermediate. It becomes vanishingly small for large energy separations, as in fluorinated groups. This is consistent with a model assuming resonant tunneling through some small density of states within the HOMO–LUMO gap of the adsorbate, since one may expect that the density of states derived from the molecule, taken at the Fermi level, increases as the gap between the HOMO (or LUMO) and the Fermi level decreases, and/or the coupling between substrate and adsorbate increases. Finally, the introduction of an external electric field can enhance the interaction between the electronic states in the complex, this effect being stronger when the energy separation is small.

It must be stressed here that our theoretical approach can only provide a qualitative interpretation of the experimental data since: (i) we do not consider explicitly the presence of the tip, (ii) the exact structure of the tip can vary from experiment to experiment, and (iii) the strength of the electric field in the tunneling junction is not known precisely. Therefore, the values of the electric field for which the calculations predict a state crossing cannot be directly correlated to the bias needed to image a given molecule or group. Despite these limitations, we consider that this theoretical study of van der Waals complexes provides a useful guideline for the understanding of the STM imaging of molecular adsorbates on graphite. In this context, it is interesting to note that the calculations on the fluorinated compounds that indicate a very weak contrast around the fluorine functionalities were performed before any STM data were taken on such systems; the experimental data subsequently fully confirmed the theoretical predictions.¹⁶

ACKNOWLEDGMENTS

The work on carbon/polymer interfaces in Mons is partly supported by the Belgian Government SSTC ‘‘Pôle d’Attraction Interuniversitaire en Chimie Supramoléculaire et Catalyse’’, FNRS/FRFC, and an IBM Academic Joint Study. The collaboration in this work has been supported by the European Commission through the ESPRIT Basic Research TOPFIT (7282). R.L. is a senior researcher with Fonds National de la Recherche Scientifique, Belgium.

- ¹S. Chiang, in *Scanning Tunneling Microscopy II*, edited by H.-J. Güntherodt and R. Wiesendanger (Springer, Berlin, 1992).
- ²J. Frommer, *Angew. Chem. Int. Ed. Engl.* **31**, 1298 (1992).
- ³J. P. Rabe, *Ultramicroscopy* **42–44**, 41 (1992).
- ⁴G. C. McGonigal, R. H. Bernhardt, and D. J. Thomson, *Appl. Phys. Lett.* **57**, 28 (1990).
- ⁵J. P. Rabe and S. Buchholz, *Science* **253**, 424 (1991).
- ⁶R. Hentschke, B. L. Schürmann, and J. P. Rabe, *J. Chem. Phys.* **96**, 6213 (1992).
- ⁷L. Askadskaya and J. P. Rabe, *Phys. Rev. Lett.* **69**, 1395 (1992).
- ⁸J. P. Rabe, S. Buchholz, and L. Askadskaya, *Phys. Scr.* **T49**, 260 (1993).
- ⁹S. Buchholz and J. P. Rabe, *Angew. Chem. Int. Ed. Engl.* **31**, 189 (1992).
- ¹⁰J. K. Spong, H. A. Mizes, L. J. LaComb, Jr., M. M. Dovek, J. E. Frommer, and J. S. Foster, *Nature* **338**, 137 (1989).
- ¹¹D. P. E. Smith, J. K. H. Hörber, G. Binnig, and H. Nejjoh, *Nature* **334**, 641 (1990).
- ¹²L. Askadskaya, C. Boeffel, and J. P. Rabe, *Ber. Bunsenges. Phys. Chem.* **97**, 517 (1993).
- ¹³J. P. Rabe and S. Buchholz, *Phys. Rev. Lett.* **66**, 2096 (1991).
- ¹⁴A. Stabel, P. Herwig, K. Müllen, and J. P. Rabe, *Angew. Chem. Int. Ed. Engl.* **34**, 1609 (1995).
- ¹⁵J. P. Rabe, S. Buchholz, and L. Askadskaya, *Synth. Metals* **54**, 339 (1993).
- ¹⁶A. Stabel, L. Dasaradhi, D. O’Hagan, and J. P. Rabe, *Langmuir* **11**, 1427 (1995).
- ¹⁷C. Ludwig, B. Gompf, W. Glatz, J. Petersen, W. Eisenmenger, M. Möbius, U. Zimmermann, and N. Karl, *Z. Physik B* **86**, 397 (1992).
- ¹⁸P. E. Burrows, Y. Zhang, E. I. Haskal, and S. R. Forrest, *Appl. Phys. Lett.* **61**, 2417 (1992).
- ¹⁹P. H. Lippel, R. J. Wilson, M. D. Miller, Ch. Wöll, and S. Chiang, *Phys. Rev. Lett.* **62**, 171 (1989).
- ²⁰G. Lambin, M. H. Delvaux, A. Calderone, R. Lazzaroni, J. L. Brédas, T. C. Clarke, and J. P. Rabe, *Mol. Cryst. Liq. Cryst.* **235**, 75 (1993).
- ²¹D. M. Eigler, P. S. Weiss, E. K. Schweizer, and N. D. Lang, *Phys. Rev. Lett.* **66**, 1189 (1991).
- ²²C. Joachim and J. F. Vinuesa, *Europhys. Lett.* **33**, 635 (1996).
- ²³J. L. Brédas and G. B. Street, *J. Am. Chem. Soc.* **110**, 7001 (1988).
- ²⁴J. L. Brédas and G. B. Street, *J. Chem. Phys.* **90**, 7291 (1989).
- ²⁵R. Lazzaroni, A. Calderone, G. Lambin, J. P. Rabe, and J. L. Brédas, *Synth. Met.* **41–43**, 525 (1991); A. Calderone, R. Lazzaroni, and J. L. Brédas, *Synth. Met.* **82**, 225 (1996).
- ²⁶S. Suzuki, P. G. Green, R. E. Bumgarner, S. Dasgupta, W. A. Goddard, and G. A. Blake, *Science* **257**, 942 (1992).
- ²⁷M. Schauer and E. R. Bernstein, *J. Chem. Phys.* **82**, 726 (1985).
- ²⁸J. Wanna, J. A. Menapace, and E. R. Bernstein, *J. Chem. Phys.* **85**, 1795 (1986).
- ²⁹J. A. Menapace and E. R. Bernstein, *J. Chem. Phys.* **91**, 2843 (1987).
- ³⁰K. O. Bomsen, H. L. Selzle, and E. W. Schlag, *J. Chem. Phys.* **85**, 1726 (1986).
- ³¹P. Hobza, H. L. Selzle, and E. W. Schlag, *J. Am. Chem. Soc.* **93**, 5893 (1990).
- ³²J. A. Pople, M. J. Frisch, and J. E. Del Bene, *Chem. Phys. Lett.* **91**, 185 (1982).
- ³³M. Dupuis, A. Farazdel, S. P. Karna, and S. A. Malvendes, in *Moteco 90, Modern Techniques in Computational Chemistry*, edited by E. Clementi (ESCOM, Leiden, 1990), p. 277.
- ³⁴A. J. Gotch and T. S. Zwier, *J. Chem. Phys.* **96**, 3388 (1992).
- ³⁵P. Hobza, H. L. Selzle, and E. W. Schlag, *Chem. Rev.* **94**, 1723 (1994).
- ³⁶H. Nakatsuji, T. Hayakawa, and T. Yonezawa, *J. Am. Chem. Soc.* **103**, 7426 (1981).